Properties of Rat Tracheal Epithelial Cells Separated Based on Expression of Cell Surface α-Galactosyl End Groups

S. H. Randell, C. E. Comment, F. C. S. Ramaekers, and P. Nettesheim

Laboratories of Pulmonary Pathobiology and Immunotoxicology, National Institute of Environmental Health Sciences, Research Triangle Park, North Carolina and Department of Molecular Cell Biology, University of Limburg, Maastricht, The Netherlands

We used *Griffonia (bandeiraea) simplicifolia* I (GS I) lectin and flow cytometry to isolate subsets of rat tracheal epithelial cells based on the presence or absence of cell surface α-galactosyl end groups. These fractions were designated GS I–positive and –negative, respectively. Ninety-eight percent of the cells in the GS I–positive fraction expressed cell surface α-galactosyl end groups; 95% had immunocytochemically detectable keratin 14–related protein (a basal cell marker) and 98% lacked alcian blue–periodic acid-Schiff (AB-PAS)-stained cytoplasmic granules. More than 90% of the GS I–positive cells had a high nuclear-to-cytoplasm ratio, had tonofilaments, and lacked organelles characteristic of other differentiated cell types; they were thus classified as basal cells. In bioassays, the GS I–positive fraction had a colony-forming efficiency greater than or equal to that of native tracheal cell suspensions, and the cells were able to repopulate denuded tracheal grafts with ciliated, secretory, and basal cells. More than 99% of the cells in the GS I–negative fraction lacked cell surface α-galactosyl end groups, 98% did not stain for keratin 14–related protein, 54% had significant numbers of AB-PAS-stained cytoplasmic granules, and 16% were identified as ciliated cells. The GS I–negative fraction had a lower colony-forming efficiency than the GS I–positive fraction but, it too, was able to repopulate denuded tracheal grafts with a complete mucociliary epithelium. These results show that both GS I–positive and –negative cells had the potential to proliferate and differentiate into the major tracheal cell types.

It has long been supposed that, by analogy to epidermal basal cells, basal cells in the trachea and bronchi play a pivotal role as stem cells in maintenance of the mucociliary epithelium. Breuer and associates (1) recently provided data to support this concept. They pulsed hamsters with [^{3}H]thymidine and followed them for 2 wk; the autoradiographic labeling index in bronchial basal cells decreased with time, while the overall labeling index remained constant and that of secretory, ciliated, and intermediate cells increased. This suggested that the basal cells are the progenitors of the other cell types. Another important function for basal cells has been suggested by morphometric studies, which indicate that basal cells provide attachment for the columnar cells (2–4). It is widely recognized that secretory cells are highly proliferative during development and following injury (5–9). Our goal is to understand the proliferative capacity and differentiation potential of the different tracheobronchial epithelial cell types.

One approach for studying progenitor-progeny relationships in tissues is to isolate specific cell types and test their biologic properties. Previous studies of the tracheobronchial epithelium using centrifugal elutriation (10–12) and cell cloning (13) to isolate subpopulations of cells showed that tracheal basal cells from rabbits gave rise to basal, secretory, and ciliated cells, while Clara cells generated only Clara and ciliated cells. Recent studies by Johnson and colleagues (14, 15), in which flow cytometry was used to separate small, agranular cells from large, granular cells (basal cells and secretory cells, respectively), suggested that secretory cells are highly proliferative and pluripotent whereas basal cells are more restricted in their ability to grow and differentiate.

A shortcoming of all the previous studies has been the lack of specific biochemical markers for the different cell types. This has created two problems: (*1*) a reliance upon rather nonspecific parameters such as density, size, and granularity for cell-separation purposes; and (*2*) an inability to precisely define the composition of different cell subpopulations based upon unique, functionally important markers.

In order to better define the phenotypes of the cells constituting the tracheal epithelium, we made use of two bio-

(Received in original form September 21, 1990 and in revised form November 19, 1990)

Address correspondence to: Scott H. Randell, Ph.D., LPP MD D2-01, NIEHS P.O. Box 12233, Research Triangle Park, NC 27709.

Abbreviations: alcian blue–periodic acid-Schiff, AB-PAS; bovine serum albumin, BSA; colony-forming efficiency, CFE; *N*-acetylgalactosamine, galNAc; *Griffonia (bandeiraea) simplicifolia* I, GS I; phosphate-buffered saline, PBS; PBS with 1% BSA plus 0.1 mM $CaCl_2$, $MnCl_2$, and $MgCl_2$, PBS+; rat tracheal epithelial cells, RTE cells; transmission electron microscopy, TEM.

chemical markers: cell surface α-galactosyl end groups and keratin 14–related protein. The former was detected with a lectin from *Griffonia (bandeiraea) simplicifolia*, and the latter with specific monoclonal antibodies. Reports in the literature suggested that these markers were preferentially expressed by basal cells in several different types of epithelia (16–23). We used flow cytometry to sort lectin-stained rat tracheal epithelial (RTE) cells. Two highly purified, viable cell fractions were obtained: one that expressed and another that lacked cell surface α-galactosyl end groups and keratin 14–related protein. The cytochemical properties, ultrastructural characteristics, proliferative ability *in vitro*, and differentiation potential *in vivo* of both cell subpopulations were examined.

Materials and Methods

RTE cells were harvested from 8- to 12-wk-old, pathogen-free F344N rats from the National Institute of Environmental Health Sciences breeding colony as previously described (24). Experiments were conducted on six occasions using six to 12 tracheas per experiment. After overnight pronase (Sigma Chemical Co., St. Louis, MO) digestion, the cells were washed with F-12 media and were resuspended in phosphate-buffered saline (PBS) containing 1% bovine serum albumin (BSA) (Sigma) and 0.05% DNAse (Sigma), which was found to effectively dissociate large cell clumps. This and all subsequent steps up to cell culture were performed at 4° C. Cell resuspension was effected by a combination of gentle vortexing and pipette tituration. Harvested cells were counted using a hemocytometer in the presence of trypan blue (0.1%, 3 min) for determination of viability.

Flow Cytometry

The protocol for lectin staining of RTE cells was adapted from McCoy and co-workers (25). In initial experiments, the α-galactosyl end group–specific, tetravalent lectin *Griffonia (bandeiraea) simplicifolia* I (GS I) isolectin B_4 was used to stain the cells, but we noted extensive cell clumping by fluorescence microscopy and a very low event rate in the flow cytometer compared to controls even at a lectin concentration of 2 μg/ml. For these reasons, subsequent experiments were performed using a functionally monovalent α-galactosyl end group–specific isolectin. GS I lectin is a tetramer of two possible subunits, either A or B, which have an equal affinity for α-galactosyl end groups, but the A subunit has a 1,000-fold greater affinity for terminal *N*-acetylgalactosamine (galNAc) residues than does the B subunit (26, 27). Five isolectins are possible: A_4, A_3B, A_2B_2, AB_3, and B_4. GS I-A_3B isolectin in the presence of galNAc is a functionally monovalent, α-galactosyl end group–specific reagent that, by virtue of its nonagglutinating properties, is useful for flow cytometry (25). Chromatographically purified GS I-A_3B, which was a single band by Coomassie-stained polyacrylamide gel electrophoresis, was obtained from Sigma. It was biotinylated with biotin-XX-N-Hydroxysuccinimide (Calbiochem, La Jolla, CA) (28). The dissociated RTE cells were incubated in 5 to 30 μg/ml of biotinylated GS I-A_3B lectin plus 2 to 5 mM galNAc in PBS with 1% BSA plus 0.1 mM $CaCl_2$, $MnCl_2$, and $MgCl_2$ (PBS+) for 30 min. The optimal GS I-A_3B and galNAc concentrations were determined in a preliminary titration that was performed for each new batch of biotinylated GS I-A_3B lectin. Typically, concentrations of 15 μg/ml of biotinylated lectin and 5 mM galNAc were used to stain 1×10^6 cells/ml. They were washed in PBS+ and incubated for 30 min in PBS+ containing 1 μg/ml streptavidin-phycoerythrin (Calbiochem). They were washed again and resuspended at a concentration of 3×10^6 cells/ml in PBS+. Controls consisted of preincubation of the lectin with 50 mM methyl-α-D-galactopyranoside (a specific inhibitor of lectin binding to α-galactosyl end groups) or glucose or fucose (controls for nonspecific sugar inhibition) for 30 min.

Two flow cytometers were used, a FACScan and a FACS 440 (Becton Dickinson, Mountain View, CA). Typically, the FACScan was used for analyzing the cells prior to and following sorting, and the FACS 440 was used for sorting. For cell sorting with the FACS 440, a 70-μm ceramic nozzle was vibrated at a constant frequency to break up the stream. Over all experiments, vibration frequencies varied from 23.6 to 26.6 kHz. An Innova 90-5 argon laser (Coherent Inc., Palo Alto, CA) emitting at 488 nm provided light for scatter analysis and fluorescence excitation. A laser power of 100 mW was used for most sorts; however, powers as low as 20 mW and as high as 200 mW were used for some experiments to improve signal-to-noise ratio. Side scatter and phycoerythrin fluorescence data were collected through 488/10 and 575/26 mM bandpass filters, respectively. Gates overlying a display of side scatter versus log phycoerythrin fluorescence were used to make sorting decisions. As explained in RESULTS, sorting windows were set over specific subpopulations. For analysis of the cells using the FACScan, excitation and emission detection wavelengths were the same as above. An aliquot of cells was also stained with ethidium bromide to assess viability (5 μl of a 0.1 μg/ml solution of ethidium bromide was added to 0.5 ml of the cell suspension 5 min before analysis). Ten thousand ungated events (except for exclusion of very small debris, which was identified by its very low forward and side light-scatter properties) per sample were analyzed using FACScan Research software (Becton Dickinson).

For subsequent cell reanalysis by flow cytometry and for the preparation of cytocentrifuge preparations, the sorted cells were collected in PBS+. For cell culture and tracheal graft repopulation experiments (see below), an aliquot of cells collected in PBS+ was diluted into Hams' F-12 media containing 1% BSA and antibiotics and was transported to the tissue culture laboratory.

Ultrastructural Analysis of Lectin-stained Cells

As explained in RESULTS, two subpopulations of RTE cells were obtained using flow cytometry. For ultrastructural analysis and carbohydrate cytochemistry (see below), cells were sorted directly into fixative (2% glutaraldehyde, 2% freshly prepared formaldehyde in 0.1 M phosphate buffer) during three experiments (on each occasion, RTE cells from 12 tracheas were pooled before lectin staining and sorting). For transmission electron microscopy (TEM), 1×10^6 fixed cells were centrifuged (Eppendorf microfuge; 30 s), washed with 0.1 M cacodylate buffer, and postfixed with 1% OsO_4 overnight at 4° C. After washing with H_2O, the cell pellets were stained *en bloc* with 2% uranyl acetate in H_2O for 2 h and embedded in warm (45° C) 1% agar. The agar-

embedded cell pellets were processed for electron microscopy using ethanol dehydration, propylene oxide transition, and embedding in EPON. Silver interference color ultrathin sections were obtained and collected on 200 mesh grids. After collection of several grids, 25 1-μm-thick sections were made, and another set of ultrathin sections was collected. This process was repeated such that three levels of each pellet were sampled. This procedure effectively sampled the entire pellet. The sections were stained with uranyl acetate and lead citrate and examined in a JEOL 100CX electron microscope. The upper left-hand corner of the section was located, and the upper left-hand corner of the first 10 grid squares containing cells were photographed at 2,600×. These were printed on 8 × 10-inch photographic paper. Cells were classified as basal cells based upon the absence of cilia, basal bodies, Golgi, or secretory granules and the presence of tonofilaments. The criteria for ciliated and secretory cells was the presence of cilia or basal bodies, and secretory granules, respectively. The inflammatory category included lymphocytes and neutrophils. Cells that did not have any unique identifying characteristics were classified as unidentified.

Keratin Immunocytochemistry

Frozen sections of rat tracheas, and cytospin preparations of unsorted and sorted RTE cells were prepared on poly-L-lysine-coated slides and were immunocytochemically stained for a spectrum of keratins using monoclonal antibodies. The antibodies used are listed in Table 1 and described in references (29–32). The antibodies have been characterized mainly in human tissues and on blots with human keratins. Therefore, when using these antibodies on rat cells and tissues, we refer to the antigens as specific keratin-related proteins. Samples were fixed in −20° C acetone for 10 min. An indirect immunoperoxidase technique with a biotinylated rat anti-mouse immunoglobulin monoclonal second antibody (RAMOL; BioCarb, Lund, Sweden) and streptavidin–horseradish peroxidase (SA-HRP; Jackson Immunoresearch, West Grove, PA) was used. Nonspecific binding was blocked by incubation with 5% BSA in PBS. Primary and secondary antibody and SA-HRP dilutions were determined empirically and made in PBS containing 1% BSA. The slides were developed with diaminobenzidine and were counterstained with methyl green. A general survey of keratin reactivity was performed, and estimations of the percentage of positive cells for each antibody in both fractions were made. For quantitation of RCK 107 reactivity, which is specific for keratin 14–related protein, 500 cells in consecutive high power fields (1,000×) were scored from three slides of both cell fractions that stained with the antibody. Cells were scored as positive if they stained considerably stronger than background.

AB-PAS Cytochemistry

Cytospin preparations of cells from three separate sorts that were fixed as above for TEM from both GS I–positive and –negative fractions were treated with 10 mM Na borohydride (to reduce background from aldehyde fixation) and were stained with alcian blue (pH 2.5)–periodic acid-Schiff reaction (AB-PAS) and methyl green after diastase treatment. Five hundred cells in consecutive high power fields (1,000×) were scored for the presence or absence of a minimum of 20 stained granules per cell (this minimum was necessary because lysosomes in all cell types were sometimes PAS positive). The presence or absence of cilia was determined as above except that phase-contrast microscopy was used to make the cilia more plainly visible.

Cell Culture

On three separate occasions, unstained RTE cells (prior to lectin staining), presorted RTE cells (stained but not sorted), and cells from both GS I–positive and –negative fractions were tested for colony-forming efficiency (CFE) as previously described (33). Cells were suspended in complete serum-free media (33) and were counted in a hemocytometer to determine viability. In triplicate, 1 × 10^4 viable cells/5 ml were seeded into 60-mm tissue culture dishes and media were changed at 24 h and at 3 and 5 d. On day 7, the dishes were fixed with ethanol, stained with Giemsa, and scored for the presence of colonies greater than 30 cells.

Tracheal Graft Repopulation Studies

Ten thousand GS I–positive and –negative cells were each inoculated into six denuded rat tracheas (tracheas from which all live cells were removed by repeated freeze-thaw cycles). These were implanted subcutaneously into rats as previously described (10–13). On day 20, these were fixed by injecting the lumen and overnight immersion in the same fixative as described above for TEM. Two specimens from each were dehydrated in ethanol and embedded in methacrylate (Historesin; LKB) according to the manufacturer's instructions. Two-micron-thick sections were stained with AB-PAS-hematoxylin.

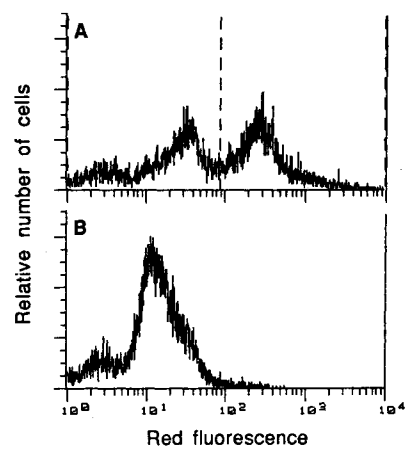

Figure 1. Histograms of red fluorescence intensity from rat tracheal epithelial (RTE) cells stained for the presence of cell surface α-galactosyl end groups with *Griffonia (bandeiraea) simplicifolia* (GS I)-A_3B lectin. (A) 51 ± 1.8% (mean ± SEM; n = 6) of the cells were highly fluorescent (to the right of the marker); these were considered to be positive for cell surface α-galactosyl end groups. (B) Preincubation of the lectin with 50 mM methyl-α-D-galactopyranoside (a sugar that specifically blocks the binding of the lectin to α-galactosyl end groups) but not with glucose or fucose (not shown) eliminated the peak of highly fluorescent cells.

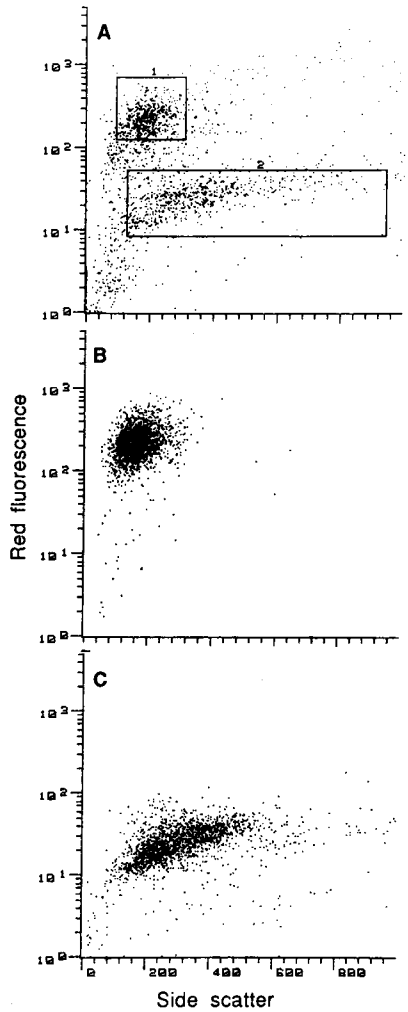

Figure 2. Two-parameter dot plots of red fluorescence versus side scatter of RTE cells stained for the presence of cell surface α-galactosyl end groups with GS I-A_3B lectin. (A) Presorted cells contained a population of highly fluorescent cells with relatively low side-scatter properties. Sorting windows were set around these cells (1) and also around less fluorescent cells with relatively high side scatter (2), although the side-scatter levels overlapped. (B) Re-run of cells from population 1 after sorting (referred to as GS I-positive fraction). (C) Re-run of cells from population 2 after sorting (referred to as GS I-negative fraction).

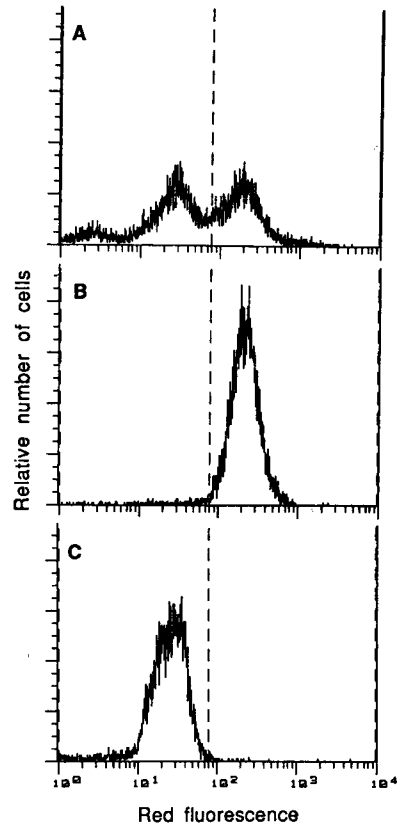

Figure 3. Histograms of red fluorescence intensity from unsorted RTE cells stained for the presence of cell surface α-galactosyl end groups with GS I-A_3B lectin (A), GS I-positive fraction (B), or GS I-negative fraction (C).

Results

Lectin Staining of Dissociated RTE Cells

To identify subsets of RTE cells expressing cell surface α-galactosyl end groups, dissociated cells were stained with GS I-A_3B lectin in the presence of *N*-acetylgalactosamine, a reaction that specifically labeled α-galactosyl end groups without agglutinating cells (see MATERIALS AND METHODS for details). Lectin that bound to the cells was detected with a red fluorochrome (phycoerythrin), and samples were run in the flow cytometer. Histograms of red fluorescence distinctly showed a bimodal fluorescence distribution (Figure 1A). A marker was placed on the graphic display at the nadir between the two major peaks, and it was calculated that 51 ± 2% (mean ± SEM, n = 6 experiments, six to 12 rats per experiment) of the total cells were highly fluorescent (i.e., contained within the peak to the right of the marker), these cells were considered to be positive for cell surface α-galactosyl end groups. Preincubation of the lectin with 50 mM methyl-α-D-galactopyranoside, which specifically inhibits lectin binding to α-galactosyl end groups, eliminated the peak containing highly fluorescent cells (Figure 1B). Fifty millimolar glucose or fucose, which were controls for nonspecific sugar inhibition, had no effect (not shown). The small peak to the very left containing events with very low fluorescence was most likely due to debris and possibly lymphocytes and erythrocytes.

Flow Cytometric Separation of Lectin-stained Cells

We used flow cytometry to purify cell subpopulations from lectin-stained RTE cells. Displays of red fluorescence versus side scatter, an indicator of granularity, of lectin-stained RTE cells showed a uniform population of highly fluorescent cells (Figure 2A). We used this display to set sorting windows over highly fluorescent cells with relatively low side scatter (Figure 2A, population 1) and over less fluorescent cells with relatively high side scatter (Figure 2A, population 2). The side scatter but not the fluorescence level of the selected populations was allowed to overlap. Cells within the high- and low-fluorescence windows were referred to as GS I-positive and -negative cells, respectively. GS I-positive and -negative cell fractions were obtained and were re-run

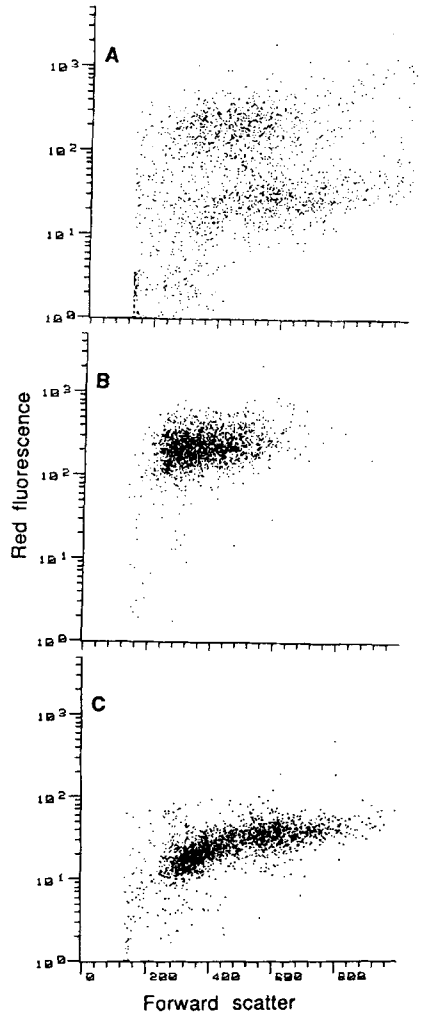

Figure 4. Two-parameter dot plots of red fluorescence versus forward scatter of unsorted RTE cells stained for the presence of cell surface α-galactosyl end groups with GS I-A_3B lectin (A), GS I-positive fraction (B); or GS I-negative fraction (C). The GS I-positive cells, on average, had lower forward scatter than the GS I-negative cells.

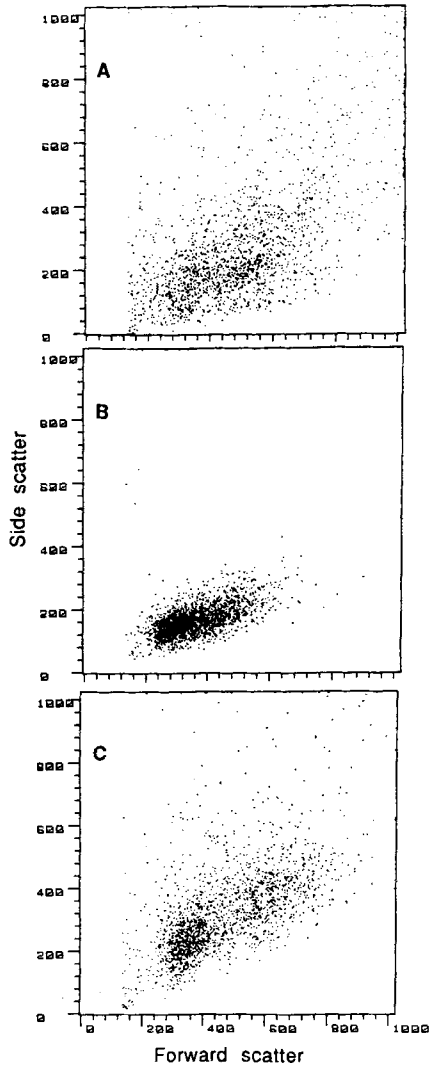

Figure 5. Two-parameter dot plots of side scatter versus forward scatter from unsorted RTE cells stained for the presence of cell surface α-galactosyl end groups with GS I-A_3B lectin (A); GS I-positive cells fraction (B); or GS I-negative cell fraction (C). Although the GS I-positive cells tended to be lower for both of these parameters, suggesting that they were relatively small and agranular, there was clearly overlap between the two sorted fractions.

in the flow cytometer as shown in Figures 2B and 2C. Typical yields for both GS I-positive and -negative cells were 20% of the total cells run in the flow cytometer, and the cell fractions appeared to be highly purified with regard to fluorescence intensity. Calculations of the purity of the fractions were performed and are displayed as histograms of red fluorescence (Figure 3). The GS I-positive fraction contained 98.4 ± 0.8% (mean ± SEM, $n = 6$) highly fluorescent cells (to the right of the marker, Figure 3B) and the GS I-negative fraction contained 99.7 ± 0.1% (mean ± SEM, $n = 6$) cells with relatively low fluorescence (to the left of the marker, Figure 3C). Ethidium bromide staining revealed that most of the events with low phycoerythrin fluorescence in the GS I-positive fraction were dead cells and debris (not shown).

Two-parameter dot plots of red fluorescence versus side scatter (Figure 2), displays of red fluorescence versus forward scatter, an indicator of cell size (Figure 4), and displays of forward scatter versus side scatter (Figure 5) indicated that the GS I-positive cells had relatively lower forward- and side-scatter properties than the GS I-negative cells. This was consistent with the GS I-positive cells being relatively small and agranular.

Viability of the Sorted Cell Fractions

To determine whether the sorted cells were suitable for subsequent culture and tracheal graft repopulation studies, we measured their viability. Cells that displayed very high levels of ethidium bromide-dependent fluorescence in the flow cytometer were considered nonviable. Cells that were used for culture and inoculation into tracheal grafts were handled somewhat differently than cells that were re-run on the flow cytometer. Because they were transported in tissue culture media containing antibiotics rather than in PBS+, we thought it necessary to measure their viability separately,

TABLE 1

Staining of cell fractions with anti-keratin antibodies

Antibody	Specificity (*keratin no.*)	GS I-positive Fraction	GS I-negative Fraction
RCK102	5 and 8	+	+++
RCK105	7	+−	++
RCK107	14	+++	+−
LL002	14	+++	+−
RGE53	18	+−	++
CK18-2	18	+	+++
LP2K	19	+	+++

Definition of abbreviations: GS I = *Griffonia (bandeiraea) simplicifolia* I; +− = < 5% positive; + = 5 to 50% positive; ++ = 50 to 95% positive; +++ = > 95% positive.

with trypan blue, as we routinely do for cell culture experiments. The results for the ethidium bromide and trypan blue methods agreed very well. The mean viability of RTE cells prior to lectin staining was 95%. The lectin-staining procedure itself caused an approximately 10% decrease in cell viability. The GS I-positive fraction contained 87 to 89% viable cells, and the GS I-negative fraction had 77 to 79% viable cells.

Keratin and AB-PAS Cytochemical Studies

To further characterize the GS I-positive and -negative cell fractions, we selected a panel of antikeratin antibodies that were known to react with specific subpopulations of epithelial cells in several tissues including the respiratory tract (34). In general, the heterotypic pair of keratins 5 and 14 are coexpressed in the basal layers of several epithelia and keratins 7, 8, 18, and 19 are so-called "luminal keratins" (35, 36). Table 1 shows estimated proportions of cells in the GS I-negative and -positive fractions that reacted with the various antibodies. Antibodies against keratin 14-related protein reacted with most of the cells in the GS I-positive fraction and with few cells in the GS I-negative fraction. Antibodies for keratins 7, 8, 18, and 19 stained more cells of the GS I-negative fraction than of the GS I-positive fraction. Based upon these results, we undertook more detailed and quantitative studies using keratin 14-related protein as a marker.

TABLE 2

*Characteristics of GS I-positive and -negative tracheal cells**

	Positive Cells (%)
GS I-positive fraction	
Keratin 14-related (RCK 107)	95 ± 2
AB-PAS	2 ± 0
Cilia	0 ± 0
GS I-negative fraction	
Keratin 14-related protein (RCK 107)	2 ± 1
AB-PAS	54 ± 1
Cilia	16 ± 4

Definition of abbreviations: GS I = *Griffonia (bandeiraea) simplicifolia* I; AB-PAS = alcian blue-periodic acid-Schiff reaction.

* Values are the mean ± SEM. Keratin 14-related protein was detected with antibody RCK 107 as described in MATERIALS AND METHODS. The presence or absence of cilia was determined using phase-contrast microscopy. Five hundred cells in consecutive high power (1,000×) fields from three slides of both cell fractions were scored. Data are based on fractions obtained from three separate experiments.

Figure 6a shows that antibody RCK 107 (specific for keratin 14-related protein) heavily stained basal cells on frozen sections of rat tracheas; Figures 6b and 6c show that almost all cells in the GS I-positive fraction and very few cells in the GS I-negative fraction, respectively, were stained with this antibody. Table 2 gives the results of cell counts with antibody RCK 107, and for comparison, the results with AB-PAS staining for diastase-resistant glycoconjugates and the percentage of ciliated cells as determined morphologically with phase-contrast microscopy. Ninety-five percent of the cells in the GS I-positive fraction stained for keratin 14-related protein compared to 2% in the GS I-negative fraction. Two percent of the cells in the GS I-positive fraction showed appreciable staining with AB-PAS, whereas > 50% of the cells in the GS I-negative fraction were AB-PAS positive. A representative example of AB-PAS-stained cell fractions is given in Figure 7. Only two out of 1,500 cells counted in the GS I-positive fraction were ciliated cells (rounded to 0%), whereas, ciliated cells comprised 16% of the GS I-negative fraction.

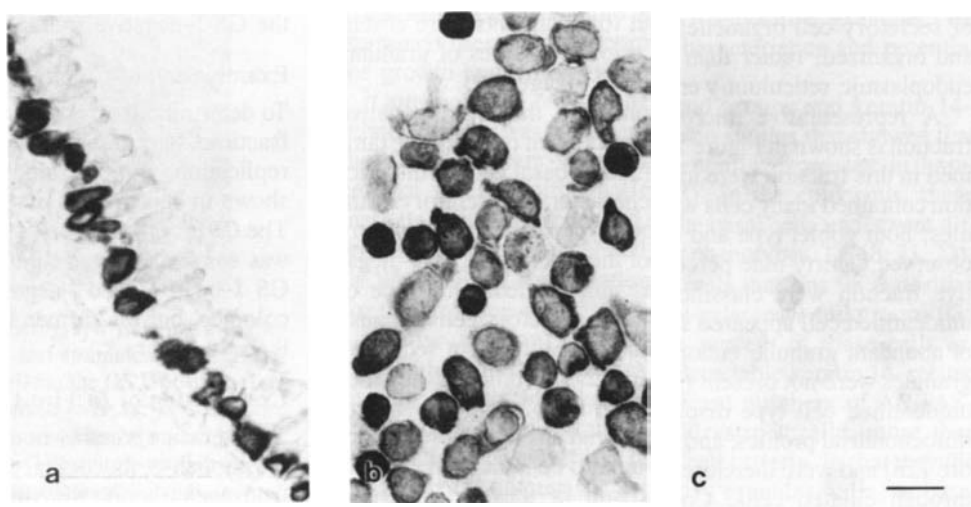

Figure 6. Immunocytochemical staining for keratin 14-related protein (antibody RCK 107) in a frozen section of the trachea (a) and on cytospin preparations of the GS I-positive fraction (b) and the GS I-negative fraction (c). Keratin 14-related protein was localized to basal cells *in vivo* and was almost exclusively contained within the GS I-positive fraction. Bar = 20 μm.

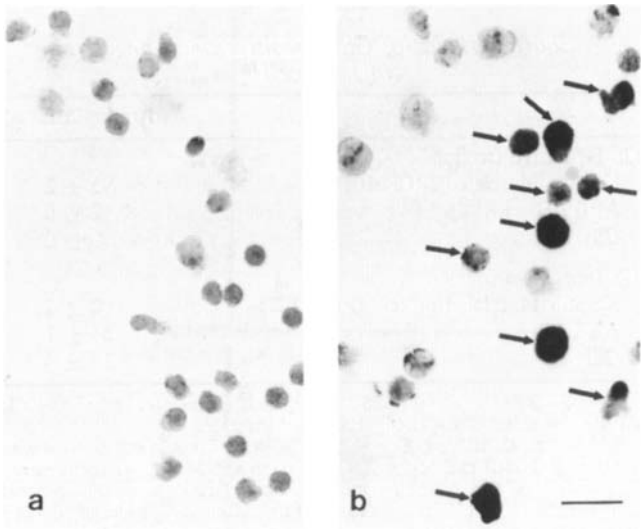

Figure 7. Cytochemical staining for glycoconjugates (alcian blue, periodic acid-Schiff reaction, methyl green counterstain) of cytospin preparations of the GS I-positive fraction (a) and the GS I-negative fraction (b). Positively stained cells (*arrows*) constituted > 50% of the GS I-negative fraction but only 2% of the GS I-positive fraction. Bar = 20 μm.

Ultrastructural Features and Differential Cell Counts of GS I-positive and -negative Cell Fractions

Ultrastructural analysis of cell pellets prepared from GS I-positive fractions showed that more than 90% of the cells were identifiable as basal cells based upon the presence of tonofilaments and the absence of organelles characteristic of ciliated or secretory cells (Figure 8; Table 3). Only one cell with characteristic secretory granules, no ciliated cells, and two inflammatory cells were observed in the > 490 cell profiles photographed. Included within the basal cell category were cells that were larger than prototypical basal cells. These had more abundant organelles such as mitochondria and endoplasmic reticulum but also contained tonofilament bundles and lacked any other distinguishing features such as Golgi or secretory granules and thus were classified as basal cells (Figure 10). We classified 8.1% of the cells in the GS I-positive fraction as unidentified. Most of them were similar to the large basal cells in that they lacked typical ciliated or secretory cell organelles, but tonofilaments were absent and organized, rather than occasional, profiles of granular endoplasmic reticulum were present (Figure 9).

A representative micrograph from the GS I-negative fraction is shown in Figure 11. Two percent of the cells examined in this fraction were identified as basal cells. This fraction contained many cells with characteristic secretory granules; both goblet type and serous type secretory cells were observed. Thirty-nine percent of the cells in the GS I-negative fraction were classified as unidentified. One type of unidentified cell appeared similar to secretory cells because of abundant granular endoplasmic reticulum, but secretory granules were not present (Figure 12a). Profiles of the other unidentified cell type displayed a lucent cytoplasm, many mitochondrial profiles, and occasional large lysosomes (Figure 12b) and were therefore thought to be nonapical sections through ciliated cells. Comparison of the ultrastructural

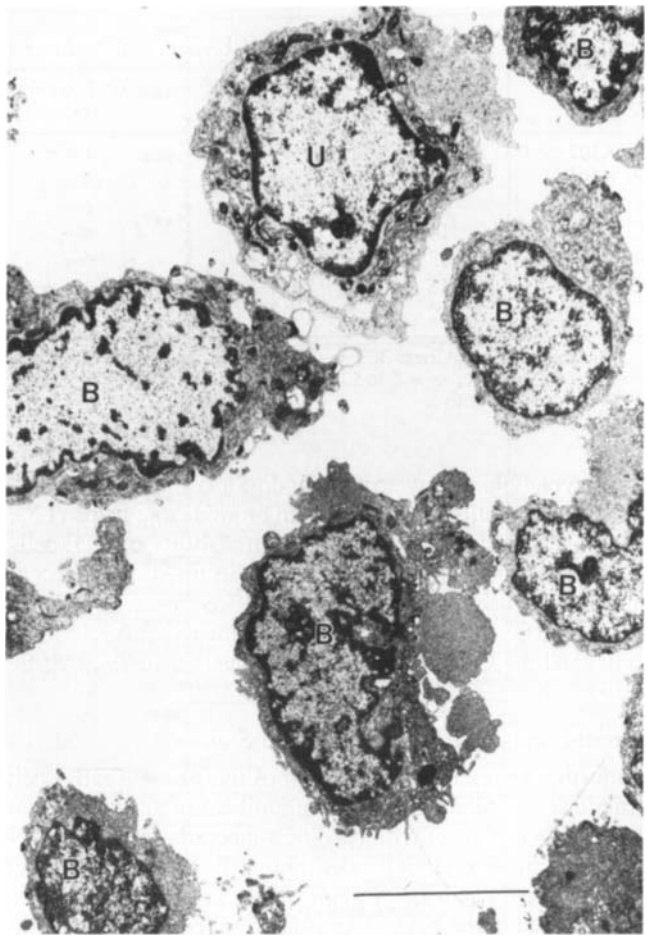

Figure 8. A representative low-power transmission electron micrograph of the GS I-positive fraction. Most of the cells in the positive fraction were classified as basal cells (B) based on the presence of tonofilaments and the lack of organelles characteristic of ciliated or secretory cells (tonofilaments may not be visible at this magnification). Eight percent of the cells in this fraction were classified as unidentified (U). A higher magnification view is shown in Figure 9. Bar = 5 μm.

differential cell count (Table 3) and the light microscopic results in Table 2 suggested that the electron microscopic methods underestimated the percentage of ciliated cells in the GS I-negative fraction.

Examination of Colony-forming Ability *In Vitro*

To determine the relative ability of the cells in the different fractions to proliferate and undergo multiple rounds of cell replication, we performed CFE assays; the data obtained are shown in Table 4. All data were corrected for cell viability. The CFE of the presorted cells (cells stained but not sorted) was somewhat lower than that of the unstained cells. Both GS I-positive and -negative fractions were able to form colonies, but the former fraction had a much greater CFE than the latter.

Examination of *In Vivo* Differentiation Potential

To determine whether both cell fractions had the capacity to reestablish a mucociliary type epithelium, 1×10^4 cells from each fraction were inoculated into tracheas from which

TABLE 3
*Ultrastructural identification of GS I-positive and -negative tracheal cells**

	% of Total Cells
GS I-positive fraction	
Basal	90.9 ± 1.7
Secretory	0.3 ± 0.4
Ciliated	None observed
Inflammatory	0.7 ± 0.6
Unidentified	8.1 ± 1.1
GS I-negative fraction	
Basal	2.1 ± 1.2
Secretory	53.7 ± 2.3
Ciliated	5.4 ± 3.5
Inflammatory	0.3 ± 0.4
Unidentified	38.5 ± 2.7

Definition of abbreviation: GS I = *Griffonia (bandeiraea) simplicifolia* I.
* Values are mean ± SEM. Cell fractions were obtained and processed for transmission electron microscopy on three separate occasions (n = 3). A total of 491 and 336 cells from GS I-positive and -negative fractions, respectively, were photographed. The inflammatory cell category included lymphocytes and neutrophils.

all live cells were removed; these were then subcutaneously transplanted to isogeneic recipients (six grafts for each fraction). Twenty days after implantation, the grafts were examined histologically (two cross sections of each graft). All of the grafts were successfully repopulated with epithelial cells.

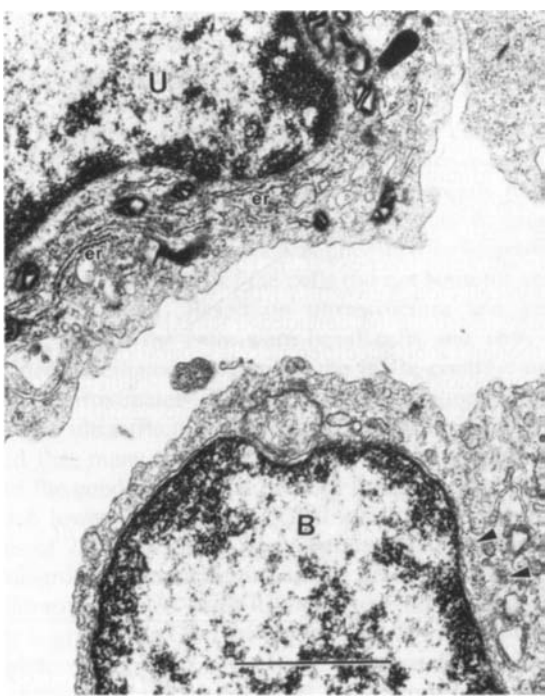

Figure 9. A transmission electron micrograph showing a higher magnification view of a basal cell (B) and an unidentified cell (U) shown in Figure 8. The unidentified cells in the GS I-positive fraction were similar to basal cells but tended to be larger with more organelles, lacked filament bundles, and had an organized pattern of granular endoplasmic reticulum (er). The more typical basal cell contains characteristic perinuclear tonofilament bundles (*arrowheads*). Bar = 1 μm.

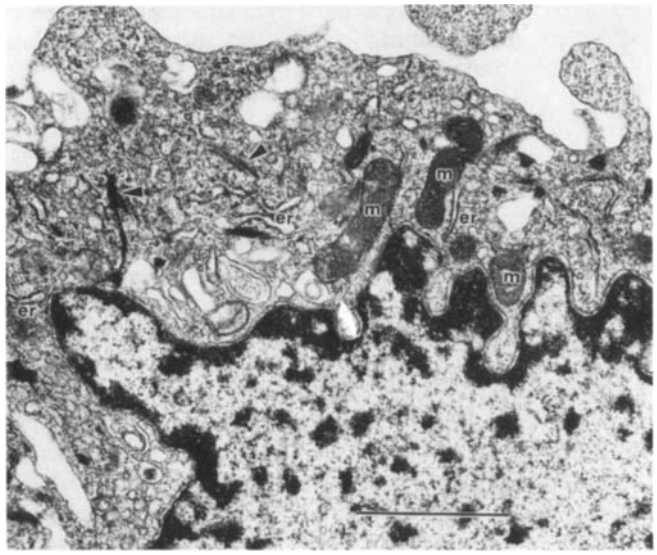

Figure 10. A representative transmission electron micrograph of a large basal cell from the GS I-positive fraction. These cells had more abundant organelles such as endoplasmic reticulum (er) and mitochondria (m) than prototypical basal cells but contained tonofilament bundles (*arrowheads*) and lacked distinguishing features such as Golgi or secretory granules. They were classified as basal cells. Bar = 1 μm.

No differences were noted in the morphology of the epithelial cells in grafts that were inoculated with either the GS I-positive or -negative cell fractions. Both contained ciliated, secretory, and basal cells; the secretory cells were principally of the goblet type and contained PAS (pink) or AB-PAS (magneta) stained granules (Figure 13).

Discussion

We used biochemical characteristics to define and obtain subsets of RTE cells. The biologic potential of these biochemically unique cell subpopulations was tested. Our specific strategy was to use flow cytometry to isolate cells based on the presence or absence of cell surface α-galactosyl end groups. The cell fractions obtained were characterized using the biochemical marker keratin 14–related protein and cytochemically detectable AB-PAS–positive granules. We examined their ultrastructural characteristics and potential for growth and differentiation.

Our choice of α-galactosyl end groups and keratin 14–related protein was predicated upon studies that showed that these two markers were preferentially expressed in basal cells of several epithelia (16–23). In the epidermis, these markers were downregulated as the basal cells underwent differentiation into the other cellular phenotypes (17, 18, 21, 22).

We obtained a population of cells that was 98% positive for the presence of cell surface α-galactosyl end groups (GS I-positive fraction). Ninety-five percent of these cells expressed immunocytochemically detectable keratin 14–related protein, and 98% lacked significant numbers of AB-PAS–stained cytoplamic granules. Ultrastructurally, more than 90% of these cells fulfilled basal cell criteria, in that they did not display characteristic secretory granules, cilia, or basal bodies; they had a high nuclear-to-cytoplasm ratio, poly-

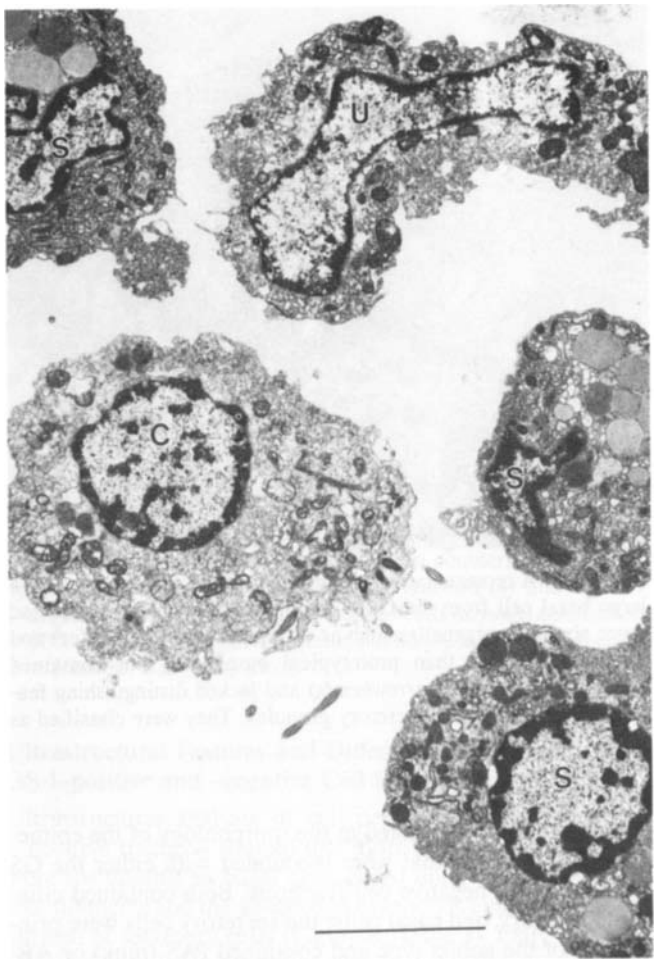

Figure 11. A representative low-power transmission electron micrograph of the GS I–negative fraction. Greater than 50% of the cells were classified as secretory cells (S) based on the presence of characteristic secretory granules. Ciliated cells (C) were also present but 39% of the cells were classified as unidentified (U). Bar = 10 μm.

ribosomes, sparse endoplasmic reticulum and mitochondria, and contained regularly identifiable perinuclear tonofilaments. Under conditions of serum-free media, the GS I–positive fraction had a CFE greater than or equal to that of native tracheal cell suspensions and the cells were able to repopulate a denuded tracheal graft with ciliated, secretory, and basal cells.

We recently reported that 37% of all cells in sections of rat tracheas were stained with an α-galactosyl end group–specific lectin (20). In the present study, using flow cytometry, we found that 51% of all cells in dissociated cell suspensions expressed cell surface α-galactosyl end groups. The reason(s) for this discrepancy is not totally clear, but previous studies showed that α-galactosyl end group–negative ciliated cells were underrepresented in protease-dissociated tracheal cell preparations (20). We also noted that the α-galactosyl end group–negative cells had a greater tendency to form clumps (unpublished observations) which would prevent them from being counted in the flow cytometer. Both of these factors could result in a higher percentage of GS I–positive cells.

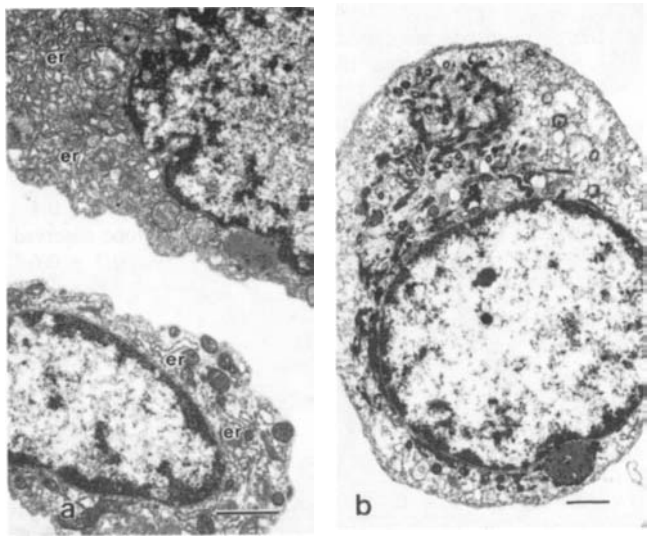

Figure 12. Transmission electron micrographs of unidentified cells from the GS I–negative fraction. (a) One type of unidentified cell appeared similar to secretory cells because of abundant endoplasmic reticulum (er), but secretory granules were not present in the plane of sectioning. (b) Profiles of another type of unidentified cell appeared to be nonapical sections through ciliated cells because of a lucent cytoplasm, abundant mitochondria, and occasional large lysosomes. Bar = 1 μm.

Most of the cells in the GS I–positive fraction had the morphologic appearance of basal cells. The fact that antibody RCK107, which is specific for keratin 14–related protein, stained only basal cells on tracheal sections and also heavily stained the GS I–positive fraction strongly supported this interpretation. Furthermore, only 2% of the cells in this fraction contained a significant number of AB-PAS–reactive secretory granules.

In previous studies, centrifugal elutriation was used to isolate small cells with ultrastructural properties of basal cells from rabbit tracheas (12). The differentiation potential of single cell clones grown *in vitro* from basal cell fractions was then tested in the denuded tracheal graft model (13). Even though rabbits, a different cell separation method, and only morphologic characterization were used in the previous studies, the conclusions were the same as in the present

TABLE 4
Colony-forming efficiency (%) of different tracheal cell fractions

	Cell Fraction			
Experiment No.	Unstained	Presorted	GS I^+	GS I^-
1	3.7	3.4	6.5 (191)*	1.5 (44)*
2	7.4	5.1	11.1 (218)*	2.2 (43)*
3	7.4	6.1	5.0 (68)*	1.1 (18)*
Mean ± SEM	6.2 ± 2.1	4.9 ± 1.4	7.5 ± 3.2	1.6 ± 0.6

Definition of abbreviations: Presorted = stained but not sorted; GS I^+ = *Griffonia (bandeiraea) simplicifolia* I (GS I)–positive cell fraction; GS I^- = GS I–negative cell fraction.

* Relative colony-forming efficiency expressed as a percentage of the colony-forming efficiency of the presorted cells. The results are the mean of triplicate samples.

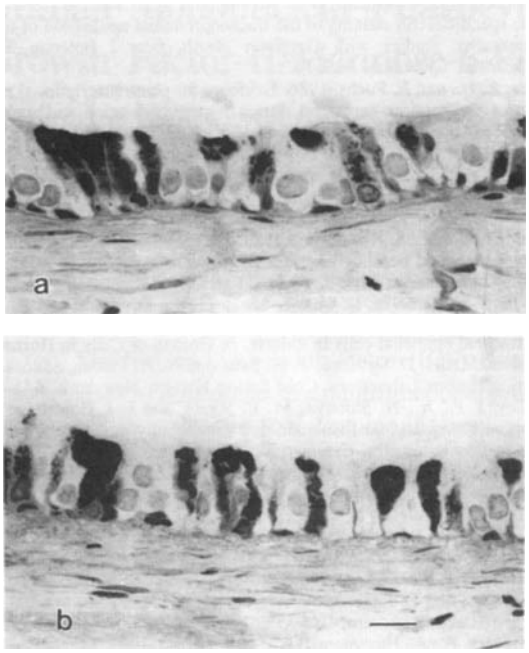

Figure 13. Two-micron-thick methacrylate sections from tracheal grafts stained with alcian blue–periodic acid-Schiff–hematoxylin. Tracheas from which all live cells were removed were inoculated with either 1×10^4 GS I–positive sorted cells (a) or 1×10^4 GS I–negative sorted cells (b) and transplanted subcutaneously into isogeneic animals. Twenty days after implantation, both sets of grafts contained ciliated, secretory, and basal cells. Bar = 20 μm.

study; namely, that cell fractions highly enriched with basal cells and practically devoid of secretory cells were able to generate secretory and ciliated cells.

In the process of sorting for GS I–positive cells, we also generated cell fractions that lacked cell surface α-galactosyl end groups. Cytochemically, 54% of these cells had significant numbers of AB-PAS–positive cytoplasmic granules (the same percentage of cells was classified as secretory by ultrastructure) and 98% of the cells did not stain for keratin 14–related protein. Based on ultrastructure and keratin staining, 2% of the cells were basal cells and 16% were identified as ciliated cells under the phase-contrast microscope. Approximately 30% of the cells remained unidentified. The ultrastructural characteristics of these cells suggested that many were pre-secretory or pre-ciliated cells. Under the conditions tested, the GS I–negative fraction had a much lower CFE than the GS I–positive fraction (mean values of 7.5% versus 1.6%, respectively). A difference of this magnitude cannot be due to the presence of 16% nonproliferative ciliated cells. Upon inoculation into denuded tracheal grafts, the GS I–negative cells also reestablished a complete mucociliary epithelium. Because the GS I–negative fraction contained very few cells expressing α-galactosyl end groups or keratin 14–related protein, we assume that the growth *in vitro* and mucociliary differentiation were accomplished by secretory or unidentified cells. More work is needed to characterize the unidentified cells and to further purify secretory cells.

Recently, Johnson and associates (14) obtained subfractions of unstained RTE cells using flow cytometry. They separated small, agranular cells from large, granular cells (basal and secretory cells, respectively). In their study, the basal cell fraction had a lower CFE than the secretory cell fraction. Another report from the same group described that the basal cell fraction repopulated denuded tracheal grafts with basal and ciliated cells, but with very few secretory cells, while the secretory cell fraction established a hypertrophic epithelial lining containing basal, ciliated, and secretory cells (15). They proposed that basal cells are competent to self-replicate and form ciliated cells while secretory cells are the major progenitors of all cell types in the trachea. These investigators also described differences in the lectin-staining pattern between basal and secretory cells. They found basal cells to react with the lectin from *Wisteria floribunda*, and to be negative for GS I (the GS I lectin used was a combination of five possible isolectins, thus it reacted with both α-galactosyl end groups and terminal *N*-acetylgalactosamine residues [see MATERIALS AND METHODS for explanation]). We have no explanation for the differences in lectin-staining results, but many previous studies have shown that GS I lectin preferentially stains basal cells (16–20). The disparate findings regarding the biologic properties of the cell isolates obtained by the two laboratories suggests that the cellular composition of the fractions obtained by Johnson and associates (14, 15) was fundamentally different than ours.

Tracheal cell suspensions from rats (and rabbits) contain from 1 to 10% cells that are clonogenic in the CFE assay, varying within this range between experiments. No cell fractionation method to date, including centrifugal elutriation (13), density gradient centrifugation (unpublished data), or flow cytometric sorting (this study and 14) has succeeded in producing a population significantly enriched with clonogenic cells. Thus, none of the biophysical or biochemical parameters used to date were specific for clonogenic cells. It is possible that the clonogenicity of the cells was grossly underestimated due to the culture conditions used in the CFE assay. Similarly, it is possible that only a small fraction of the cells we isolated were responsible for repopulating denuded tracheal grafts with a mucociliary epithelium. We plan to continue our efforts to identify and isolate clonogenic cells and cells with stem cell–like functions from tracheas.

In summary, we obtained highly purified, viable subpopulations of RTE cells that expressed or lacked cell surface α-galactosyl end groups. By immunochemical, cytochemical and ultrastructural criteria, the fractions were enriched with basal cells and secretory cells, respectively. We showed that clonogenic ability as well as broad differentiation potential are properties of both basal cell– and non-basal cell–enriched fractions. This may indicate that basal and secretory cells are extremely closely linked cell types. The morphologic similarity of the undifferentiated epithelium in tracheal grafts at early time points after inoculation with either cell fraction ([37], work in progress), suggests that these cells are capable of trans-differentiation. An alternative possibility that cannot be ruled out at the moment is that both cell fractions contained a small pluripotent subpopulation of cells, which escaped identification.

Acknowledgments: We thankfully acknowledge the expert assistance of Mr. Jack Vincent at the Department of Pathology Flow Cytometry Facility, University of North Carolina, Chapel Hill.

References

1. Breuer, R., G. Zajicek, T. G. Christensen, E. C. Lucey, and G. L. Snider. 1990. Cell kinetics of normal adult hamster bronchial epithelium in the steady state. *Am. J. Respir. Cell Mol. Biol.* 2:51–58.
2. Evans, M. J., and C. G. Plopper. 1988. The role of basal cells in adhesion of columnar cells to airway basement membrane. *Am. Rev. Respir. Dis.* 138:481–483.
3. Evans, M. J., R. A. Cox, S. G. Shami, B. Wilson, and C. G. Plopper. 1989. The role of basal cells in attachment of columnar cells to the basal lamina of the trachea. *Am. J. Respir. Cell Mol. Biol.* 1:463–469.
4. Evans, M. J., R. A. Cox, S. G. Shami, B. Wilson, and C. G. Plopper. 1990. Junctional adhesion mechanisms in airway basal cells. *Am. J. Respir. Cell Mol. Biol.* 3:341–347.
5. McDowell, E. M., C. Newkirk, and B. Coleman. 1985. Development of hamster tracheal epithelium. I. A quantitative morphologic study in the fetus. *Anat. Rec.* 213:429–447.
6. McDowell, E. M., C. Newkirk, and B. Coleman. 1985. Development of hamster tracheal epithelium. II. Cell proliferation in the fetus. *Anat. Rec.* 213:448–456.
7. Plopper, C. G., J. Alley, and A. J. Weir. 1986. Differentiation of tracheal epithelium during fetal lung maturation in the rhesus monkey *Macaca mulatta*. *Am. J. Anat.* 176:59–71.
8. Keenan, K. P., T. S. Wilson, and E. M. McDowell. 1983. Regeneration of hamster tracheal epithelium after mechanical injury. IV. Histochemical, immunocytochemical and ultrastructural studies. *Virchows Arch. [B]* 43:213–240.
9. McDowell, E. M., K. P. Keenan, and M. Huang. 1984. Effects of vitamin A–deprivation in hamster tracheal epithelium: a quantitative morphologic study. *Virchows Arch. [B]* 45:197–219.
10. Brody, A. R., G. E. R. Hook, G. S. Cameron, A. M. Jetten, C. J. Butterick, and P. Nettesheim. 1987. The differentiation capacity of Clara cells isolated from the lungs of rabbits. *Lab. Invest.* 57:219–229.
11. Hook G. E. R., A. R. Brody, G. S. Cameron, A. M. Jetten, L. B. Gilmore, and P. Nettesheim. 1987. Repopulation of denuded tracheas by Clara cells isolated from the lungs of rabbits. *Exp. Lung Res.* 12:311–329.
12. Inayama, Y., G. E. R. Hook, A. R. Brody *et al.* 1988. The differentiation potential of tracheal basal cells. *Lab. Invest.* 58:706–717.
13. Inayama, Y., G. E. R. Hook, A. R. Brody, A. M. Jetten, T. Gray, J. Mahler, and P. Nettesheim. 1989. *In vitro* and *in vivo* growth and differentiation of clones of tracheal basal cells. *Am. J. Pathol.* 134:539–549.
14. Johnson, N. G., J. S. Wilson, R. Habbersett, D. G. Thomassen, G. M. Shopp, and D. M. Smith. 1990. Separation and characterization of basal and secretory cells from the rat trachea by flow cytometry. *Cytometry* 11:395–405.
15. Johnson, N. G., A. F. Hubbs, and D. G. Thomassen. 1989. Epithelial progenitor cells in the rat respiratory tract. *In* Respiratory Carcinogenesis. D. Thomassen and P. Nettesheim, editors. Hemisphere Publishing, New York. 88–98.
16. Peters, B. P., and I. J. Goldstein. 1979. The use of fluorescein-conjugated *Bandeiraea simplicifolia* B4-isolectin as a histochemical reagent for the detection of α-D-galactopyranosyl groups. *Exp. Cell Res.* 120:321–334.
17. Brabec, R. K., B. P. Peters, I. A. Bernstein, R. H. Gray, and I. J. Goldstein. 1980. Differential lectin binding to cellular membranes in the epidermis of the newborn rat. *Proc. Natl. Acad. Sci. USA* 77:477–479.
18. Zieske, J. D., and I. A. Bernstein. 1982. Modification of cell surface glycoprotein: addition of fucosyl residues during epidermal differentiation. *J. Cell Biol.* 95:626–631.
19. Flint, F. F., B. A. Schulte, and S. S. Spicer. 1986. Glycoconjugate with terminal α galactose. *Histochemistry* 84:387–395.
20. Shimizu, T., P. Nettesheim, J. G. Mahler, and S. H. Randell. 1991. Cell-type specific lectin staining of the tracheobronchial epithelium of the rat: quantitative studies with *Griffonia simplicifolia* I isolectin B4. *J. Histochem. Cytochem.* 39:7–14.
21. Tyner, A. L., and E. Fuchs. 1986. Evidence for posttranscriptional regulation of the keratins expressed during hyperproliferation and malignant transformation in human epidermis. *J. Cell Biol.* 103:1945–1955.
22. Vassar, R., M. Rosenberg, S. Ross, A. Tyner, and E. Fuchs. 1989. Tissue-specific and differentiation-specific expression of a human K14 keratin gene in transgenic mice. *Proc. Natl. Acad. Sci. USA* 86:1563–1567.
23. Wetzels, R. H. W., R. Holland, U. J. G. M. van Haelst, E. B. Lane, I. M. Leigh, and F. C. S. Ramaekers. 1989. Detection of basement membrane components and basal cell keratin 14 in noninvasive and invasive carcinomas of the breast. *Am. J. Pathol.* 134:571–579.
24. Wu, R., J. W. Groelke, L. Chang, M. E. Porter, D. Smith, and P. Nettesheim. 1982. Effects of hormones on the multiplication and differentiation of tracheal epithelial cells in culture. *In* Growth of Cells in Hormonally Defined Media. D. Sirbasku, F. H. Sata, and N. A. Pardee, editors. Cold Spring Harbor Laboratory, Cold Spring Harbor, New York. 641–656.
25. McCoy, J. P., Jr., N. Shibuya, M. C. Riedy, and I. J. Goldstein. 1986. *Griffonia simplicifolia* I isolectin as a functionally monovalent probe for use in flow cytometry. *Cytometry* 7:142–146.
26. Murphy, L. A., and I. J. Goldstein. 1977. The five alpha-D-galactopyranosyl-binding isolectins from *Bandeiraea simplicifolia* seeds. *J. Biol. Chem.* 252:4739–4742.
27. Goldstein, I. J., D. A. Blake, S. Ebisu, T. J. Williams, and L. A. Murphy. 1981. Carbohydrate binding studies on the *Bandeiraea simplicifolia* I isolectins. *J. Biol. Chem.* 256:3890–3893.
28. Harlow, E., and D. Lane. 1988. Antibodies: A Laboratory Manual. Cold Spring Harbor Laboratory, Cold Spring Harbor, New York. 341.
29. Ramaekers, F., A. Huysmans, O. Moesker *et al.* 1983. Monoclonal antibody to keratin filaments specific for glandular epithelia and their tumors: use in surgical pathology. *Lab. Invest.* 49:353–361.
30. Broers, J. L. V., D. N. Carney, J. K. Rot *et al.* 1986. Intermediate filament proteins in classic and variant types of small cell lung carcinoma cell lines: a biochemical and immunochemical analysis using a panel of monoclonal and polyclonal antibodies. *J. Cell Sci.* 83:37–60.
31. Purkis, P. E., J. B. Steel, I. C. McKenzie, W. B. J. Nathrath, I. M. Leigh, and E. B. Lane. 1990. Antibody markers of basal cells in complex epithelial. *J. Cell Sci.* 97:39–50.
32. Wetzels, R. H. W., H. J. H. Kuypers, E. B. Lane *et al.* 1991. Basal cell-specific and hyperproliferation-related keratins in human breast cancer. *Am. J. Pathol.* 138:751–763.
33. Thomassen, D. G., U. Saffiotti, and M. E. Kaighn. 1986. Clonal proliferation of rat tracheal epithelial cells in serum-free medium and their responses to hormones, growth factors and carcinogens. *Carcinogenesis* 7:2033–2039.
34. Rutten, A. A. J. J. L., J. P. Bruyntjes, and F. C. S. Ramaekers. 1988. Intermediate filament expresion in normal and vitamin A depleted cultured hamster tracheal epithelium as detected by monoclonal antibodies. *Virchows Arch. [B]* 56:103–110.
35. Moll, R., W. W. Franke, D. L. Schiller, B. Geiger, and R. Krepler. 1982. The catalog of human cytokeratins: patterns of expression in normal epithelia, tumors and cultured cells. *Cell* 31:11–24.
36. Cooper, D., A. Schermer, and T-T. Sun. 1985. Classification of human epithelia and their neoplasms using monoclonal antibodies to keratins: strategies, applications, and limitations. *Lab. Invest.* 52:243–256.
37. Randell, S. H., T. Shimizu, and P. Nettesheim. 1991. *In vivo* differentiation of rat tracheal epithelial (RTE) cell subpopulations. *Am. Rev. Respir. Dis.* 143(Suppl.):A146. (Abstr.)